

Charge transfer across the As/Si(100)-2×1 interface

J. A. Evans, A. D. Laine, and P. Weightman

*Department of Physics, University of Liverpool, Liverpool, United Kingdom
and Surface Science Research Centre, University of Liverpool, Liverpool L69 3BX, United Kingdom*

J. A. D. Matthew

Department of Physics, University of York, Heslington, York YO1 5DD, United Kingdom

D. A. Woolf, D. I. Westwood, and R. H. Williams

Department of Physics, University College of Wales, Cardiff, United Kingdom

(Received 15 July 1991)

A high-performance Auger spectrometer has been used to separate the bulk and interface contributions to the Auger spectra of the As/Si(100) interface. Combining these results with measurements of the photoelectron spectra of core levels shows that the Auger-parameter shifts between atoms at the interface and in the bulk elements are -0.64 ± 0.04 eV for As and 0.68 ± 0.04 eV for Si. The Auger-parameter shifts are analyzed in terms of recent theoretical models that indicate that there is a small charge transfer of $\sim 0.2e$ from Si to As at the interface.

I. INTRODUCTION

The termination of single-crystal surfaces of Si by a monolayer of As atoms is an important step in attempts to grow GaAs epitaxially on Si.¹⁻⁴ The physical structures of As/Si(111) and As/Si(100) surfaces are well understood⁵⁻⁸ and there is increasing interest in their electronic structures.⁹⁻¹⁴ In this work we report measurements of the Auger parameter shift between atoms at the As/Si(100) interface and in the elemental solids. The results of these measurements are analyzed in terms of recent theoretical approaches¹⁵⁻¹⁷ and this indicates that there is a small charge transfer of $\sim 0.2e$ from Si to As atoms at the interface.

II. EXPERIMENT

Low-resistivity *n*-type (0.006–0.015 Ω/cm , Sb doped) 3-in.-diam Si(100) substrates were employed in this study. Each wafer was chemically etched according to a simple, one cycle, HF acid and HCl:H₂O₂:H₂O (1:7:1) reoxidation routine.¹⁸ After In-free mounting onto a Mo platter, each substrate was admitted, via a load-lock, into the preparation chamber of a VG semicon V80H molecular-beam epitaxy (MBE) reactor based in the Cardiff laboratory. Samples were then out gased for ~ 3 h at $\sim 300^\circ\text{C}$ and then transferred into the growth chamber of the MBE system. Experimental details concerning the substrate temperature calibrations and MBE flux measurements have been reported earlier.^{18,19} *In situ* reflection high-energy electron diffraction (RHEED) was used to characterize the Si substrate surface throughout the growth process. The substrate was annealed for half an hour at $\sim 850^\circ\text{C}$. During this anneal the initial (1×1) RHEED pattern associated with the thin volatile oxide layer covering the substrate surface¹⁸ transformed into a sharp well-defined (2×1) double domain reconstruction

indicating the desorption of the oxide layer. Following this anneal the sample was allowed to cool. Within the $850^\circ\text{C} > T > 120^\circ\text{C}$ temperature range this cooling process was affected in an incident As₄ flux of $\sim 4.5 \times 10^{14}$ molecules $\text{cm}^{-2}\text{s}^{-1}$. As the substrate temperature passed through the desorption temperature of As/Si ($\sim 700^\circ\text{C}$) the RHEED features of the (2×1) double domain pattern elongated, corresponding to the uptake of a monolayer of As. On achieving a temperature of 120°C the As₄ flux was shuttered and the substrate allowed to continue cooling until the sample thermocouple read its lower limit temperature, -10°C . The complete cooling process from 850°C to -10°C typically took ~ 5.25 h. Once the substrate had reached -10°C the deposition of an amorphous As cap was initiated by opening the effusion cell shutter and As₄ was deposited for ~ 1 h. Post-growth RHEED observations confirmed the As overlayer to be amorphous in nature.

The As capped As/Si(100) crystal was removed from the Cardiff growth chamber and mounted in a high-sensitivity Auger electron spectrometer recently completed by the Liverpool group. This instrument is equipped with a high power (2 kW) Mo anode bremsstrahlung x-ray source, a monochromated Al *K* α x-ray source and low-energy electron diffraction. Operating pressures for these experiments were in the low 10^{-10} mbar ranges.

The experiments were designed to measure the change in the Auger parameter α of each element between the elemental materials and the atoms at the As/Si(100) interface. As discussed earlier,^{15,16} $\Delta\alpha$ can be accurately determined from measurements of environmental changes in the core-level ionization energies I and the kinetic energies of core-core-core Auger transitions K according to

$$\Delta\alpha = \Delta I + \Delta K . \quad (1)$$

An important feature of Eq. (1) is that systematic errors in the determination of ΔI and ΔK , which arise from referencing the energy scale of the instrument, cancel in the determination of $\Delta\alpha$. Measurements of the $2p$ photoelectron and $L_3M_{4,5}M_{4,5}$ Auger spectra of elemental As were performed on the As cap of the specimen after this had been cleaned of contaminants by slight resistive heating of the specimen to $\sim 300^\circ\text{C}$ to remove the surface layer. This left a clean layer of As which, since no x-ray photoelectron spectroscopy (XPS) or Auger signal could be observed from the underlying Si, was estimated from electron escape depths²⁰ to have a thickness $> 280 \text{ \AA}$. Subsequent more prolonged resistive heating of the Si crystal at $\sim 300^\circ\text{C}$ removed all the As except the final monolayer coverage and this As/Si(100) surface gave a standard 2×1 LEED pattern.¹⁰ The As and Si $2p$ photoelectron spectra and the As $L_3M_{4,5}M_{4,5}$ and Si $KL_{2,3}L_{2,3}; ^1D_2$ Auger spectra were then measured for the As/Si(100) surface. The photoelectron spectra were excited by monochromated Al $K\alpha$ x rays with an instrumental resolution of $\sim 0.5 \text{ eV}$. The Auger spectra were recorded with an instrumental resolution of 0.07 eV . Due to the large escape depth of electrons at these energies²⁰ the photoelectron and Auger electron spectra of Si obtained from the As/Si(100) surface are dominated by contributions from bulk Si. In order to separate the bulk and surface contributions to the Si spectra measurements were made with the plane of the specimen surface normal and also at steep angles to the axis of the electron lens.

III. RESULTS

The spectra of the As $2p_{3/2}$ photoelectron lines and $L_3M_{4,5}M_{4,5}$ Auger transitions are shown in Figs. 1 and 2, respectively. The results obtained for elemental As are shown by full lines and those obtained from the As/Si(100) interface by the dots. The profile of the As $L_3M_{4,5}M_{4,5}$ Auger transitions is well understood,^{21,22} the main peak arising from a combination of an intense 1G component and, rather weaker, 3P and 1D components of the final-state $3d^8$ multiplet structure. The energy scale for these figures is that of the spectrometer. Since we are only interested in the relative shifts in the position of the peaks, these can be determined accurately and are shown in Table I. It may be noted that the Auger profile obtained for As atoms at the As/Si(100) interface is nar-

TABLE I. Measured changes in core-level binding energies, Auger kinetic energies, and Auger parameters between the As/Si(100) interface and the pure elements. All values are in eV.

	As/Si(100)-As	As/Si(100)-Si
ΔI (As; $2p$)	-0.12 ± 0.03	
ΔI (Si; $2p$)		$+0.45 \pm 0.03$
ΔK (As; $L_3M_{4,5}M_{4,5}$)	-0.52 ± 0.03	
ΔK (Si; $KL_{2,3}L_{2,3}; ^1D_2$)		$+0.23 \pm 0.04$
$\Delta\alpha$ (As)	-0.64 ± 0.04	
$\Delta\alpha$ (Si)		$+0.68 \pm 0.04$
$\Delta\beta$ (As)	-0.88 ± 0.2	
$\Delta\beta$ (Si)		$+1.58 \pm 0.2$

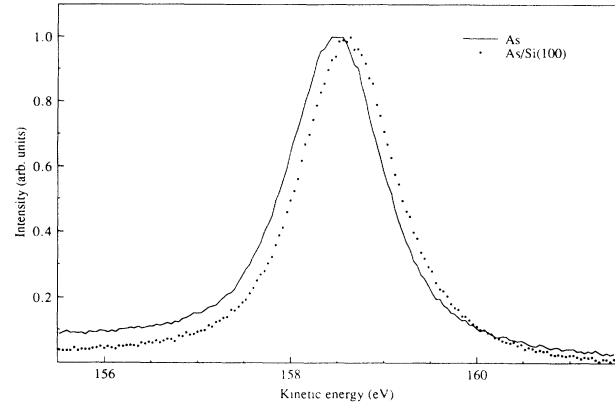


FIG. 1. Comparison of the As $2p_{3/2}$ photoelectron line for pure As (line) and As at the Si(100)/As interface.

rower than that obtained for elemental As.

The Si $2p$ photoelectron spectra and $KL_{2,3}L_{2,3}; ^1D_2$ Auger spectra obtained with the As/Si(100) surface at an angle of 85° to the axis of the electron lens are shown by the dots in Fig. 3(a) and the crosses in Fig. 4, respectively. The spectra shown by the dots in Fig. 3(b) and by the squares in Fig. 4 were obtained with the As/Si(100) surface at angles of 30° and 15° to the axis of the electron lens, respectively. The difference in core-level ionization energies ΔI between bulk Si and Si at the As/Si(100) interface has been measured previously² in photoemission experiments employing synchrotron radiation to optimize the surface sensitivity of the experiment. The previous work² showed that the $2p$ core levels of Si atoms at the As/Si(100) interface are shifted 0.45 eV higher in binding energy than the $2p$ core levels of bulk Si and this result is included in Table I. The lower resolution of our photoemission experiments and the dominance of the bulk con-

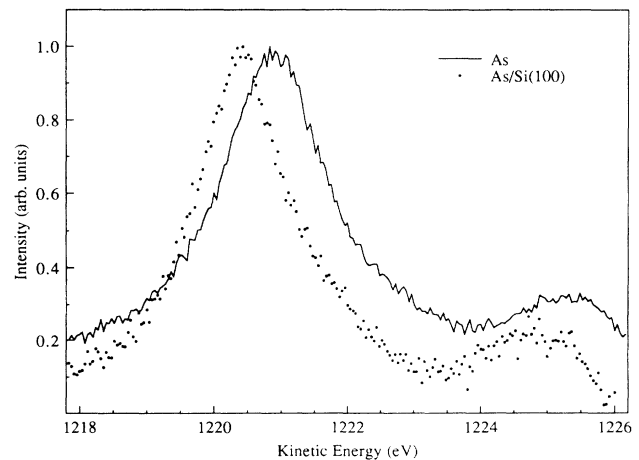


FIG. 2. Comparison of the As $L_3M_{4,5}M_{4,5}$ for solid As (line) and As at the Si(100)/As interface. The main peak is a combination of the 1G , 3P , and 1D components of the $3d^8$ multiplet structure. The weaker feature to high kinetic energy is due to the 3F component of the multiplet structure.

tribution means that we cannot determine the surface to bulk shift with the same accuracy as in the previous work, but we can use the previous results to check the consistency of our measurements and determine the fraction of the Si signal arising from interface Si which will be a useful check on the analysis of the Si Auger profiles. The lines in Fig. 3 are calculated spectra obtained from an envelope of the contribution from spin-orbit-split components of the $2p$ photoemission of bulk and interface Si. In simulating the spectra the $2p$ spin-orbit splitting of Si (0.6 eV) and the relative intensity of the spin-orbit components (1:2) were combined with the separation of the bulk and interface contributions measured in the previous work.² The fractional contribution to the signal arising from interface Si was obtained from

$$f_{\theta} = 1 - \exp(-D/\lambda \cos\theta) = R_{\theta}/(1 + R_{\theta}), \quad (2)$$

where R_{θ} is the ratio of surface and bulk intensities, D is the thickness of the surface layer, and θ is the takeoff angle. The calculated profiles were convoluted with a Gaussian of full width half maximum (FWHM) of 0.5 eV,

corresponding to the spectrometer resolution and a weak background proportional to the total signal strength to higher kinetic energy was added to the calculated profiles. The simulated spectral profiles were fitted simultaneously to the experimental data of Figs. 3(a) and 3(b). The only free parameters in these fits were the values of R_{θ} and the background, the latter having only a slight influence on the spectral profiles. The fits shown in Figs. 3(a) and 3(b) were obtained with $R_{85} = 0.048$ and $R_{30} = 0.101$, indicating that the interface contributions, shown shaded in the figures, amount to 5% and 10% of the spectral intensity respectively. Inserting these results into (2) yields results for D/λ of 0.048 and 0.046 the closeness of the results demonstrating the consistency of our analysis and confirming the agreement of our measurements with the previous work. Taking the escape depth at this kinetic energy²⁰ as 25.7 Å yields a value of 1.21 Å for D , which is in very good agreement with the As-Si interlayer distance at the interface (1.26 Å for the As-capped interface and 1.43 Å for the interface in air⁵).

We turn now to an analysis of the Si $KL_{2,3}L_{2,3}^1D_2$ Auger spectra shown in Fig. 4. These spectra were mea-

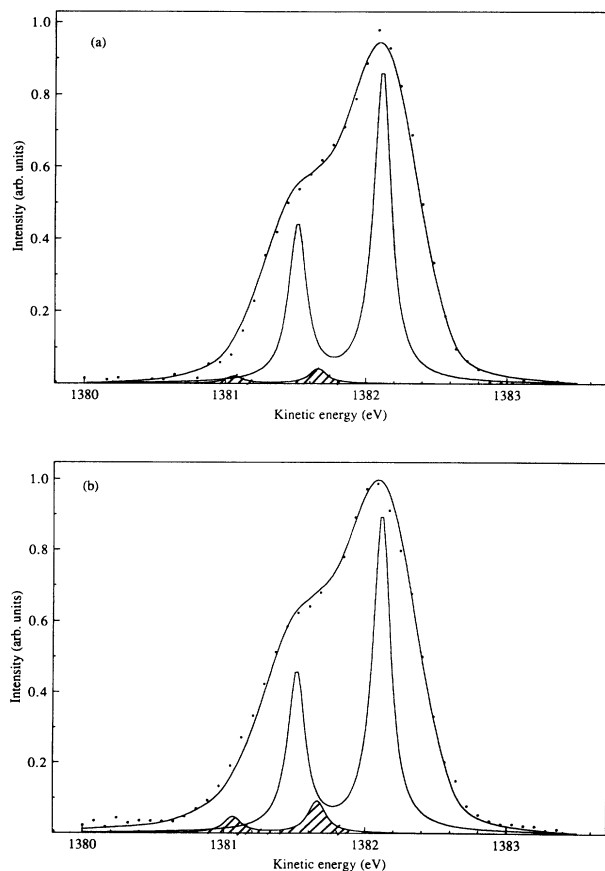


FIG. 3. Experimental spectra of the Si $2p$ photoelectron lines (dots) and theoretical fits (line), see text, for angles between the surface and the direction of the electron lens of (a) 85° and (b) 30°. The positions and relative intensities of the components to the theoretical fits are shown under the actual spectra with the interface component shaded. These components have not been corrected to allow for the instrumental broadening.

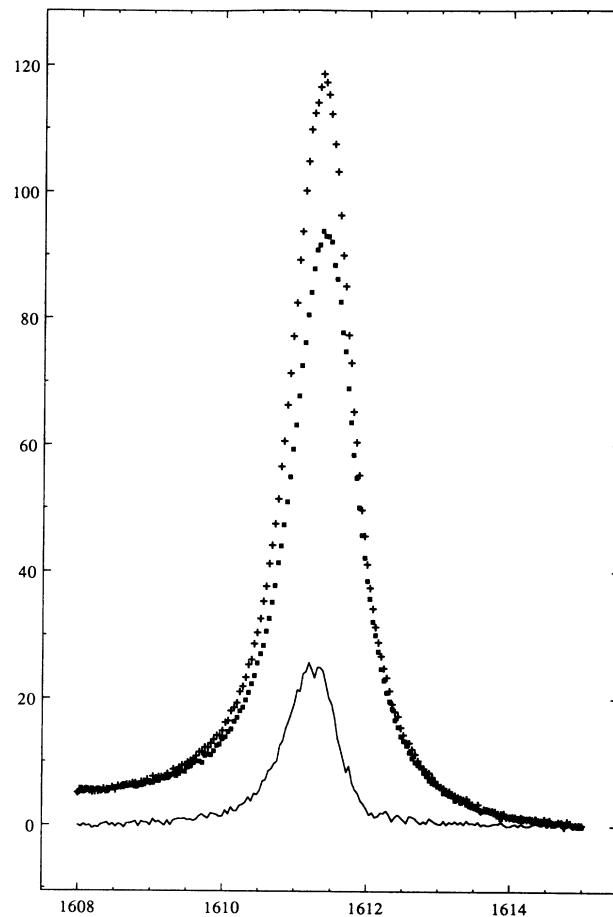


FIG. 4. Experimental spectra of the 1D component of the Si KLL Auger transition for angles between the surface and the direction of the electron lens of (a) 85° (crosses) and (b) 15° (squares). The lower curve is the result of subtracting the spectrum shown by the squares from that shown by the crosses.

sured with an instrumental resolution of 0.07 eV, which is significantly less than the expected value of the intrinsic lifetime broadening of the levels involved in the transition. The lifetime width of the initial K hole state is calculated²³ to be 0.38 eV and, although there are no calculations of the lifetime broadening of the two-hole final state [$2p^2; ^1D_2$], we do not expect this to be substantially larger than twice the width of the [$2p$] hole state,²⁴ ~ 0.02 eV, giving a total estimated lifetime contribution of < 0.5 eV. If there were no shift in the energy of the transition between bulk and interface Si, the spectra of Fig. 4 should be adequately described by a Lorentzian line of FWHM ~ 0.5 eV convoluted with a Gaussian of FWHM 0.07 eV representing the spectrometer contribution. Neither of the spectra can be fitted to a single component in this way and a close comparison of the spectral shapes suggests that each is composed of more than one component. A subtraction of the two spectral profiles shown in Fig. 4 reveals a symmetrical peak at a kinetic energy of 1611.28 ± 0.04 eV. The subtraction was performed by first removing constant backgrounds from the two spectra so that the signal at the extreme high energy of each spectrum was zero. This revealed slight differences in the background count on the extreme low-energy side of the spectra, which were $\sim 5\%$ of the peak height for the spectrum obtained at the low takeoff angle and $\sim 4\%$ for the spectrum taken at the high takeoff angle. These differences are expected given the increased surface sensitivity of spectra taken at low takeoff angles. In order to correct for the differences in background, which are not sufficient to explain the difference in shape of the two spectra, the spectra were normalized to give the same background on the low kinetic-energy side of the spectra, as shown in Fig. 4. The subtraction shows that each profile consists of two components, which we identify as a strong bulk component at 1611.28 ± 0.04 eV and a weaker interface component at higher kinetic energy.

In order to determine the difference in energy of the bulk and interface components the spectra of Fig. 4 were fitted simultaneously to two components, the width and position of which were treated as free parameters, but with the constraint that they be identical in the fits to the two data sets. The relative intensity of the two components was allowed to vary in the fit to each spectrum. The results are shown by the full curves in Fig. 5(a) for the spectra obtained by high takeoff angle and in Fig. 5(b) for the spectra taken at low takeoff angle. In each figure the experimental spectra are shown by the dots and the interface components obtained from the fitting procedure are shown shaded. The results of fitting each spectrum to two Lorentzian components does not give a perfect fit to either data set. However, it should be emphasized that the fitting procedure is very constrained by the requirement of fitting both sets of data simultaneously and that one could reasonably attribute the remaining discrepancies to uncertainty in the background contributions and to deviations of the component line shapes from Lorentzians due to phonon broadening and, in the case of the surface component, from inhomogeneous broadening arising from contributions from surface defects. The data

do not justify any detailed attempts to analyze such contributions. The crucial issue for our purposes is that the direct subtraction of the two spectra (Fig. 4) show that there are only two strong components and that this is what we expect since the photoemission data confirm that there are only two Si sites, the bulk site and the interface site. This view is confirmed by a consideration of the relative intensity of the bulk and surface components obtained from the fit. The escape depth²⁰ corresponding to this kinetic energy is 28.6 Å. Substituting this value and the relative intensity of the bulk and interface components as a function of angle, obtained from the fits, in Eq. (2) yields values of D of 1.30 and 1.34 Å for the data of Figs. 5(a) and 5(b), respectively. These values are sufficiently consistent with each other and with the results of the analysis of the Si $2p$ photoelectron spectra to provide strong confirmation of the analysis of the Auger line shapes. The procedure of requiring a simultaneous and consistent fit to the spectra taken at both takeoff angles is a strong constraint on the analysis which is particularly sensitive to the separation of the two components, the result for which is shown in Table I.

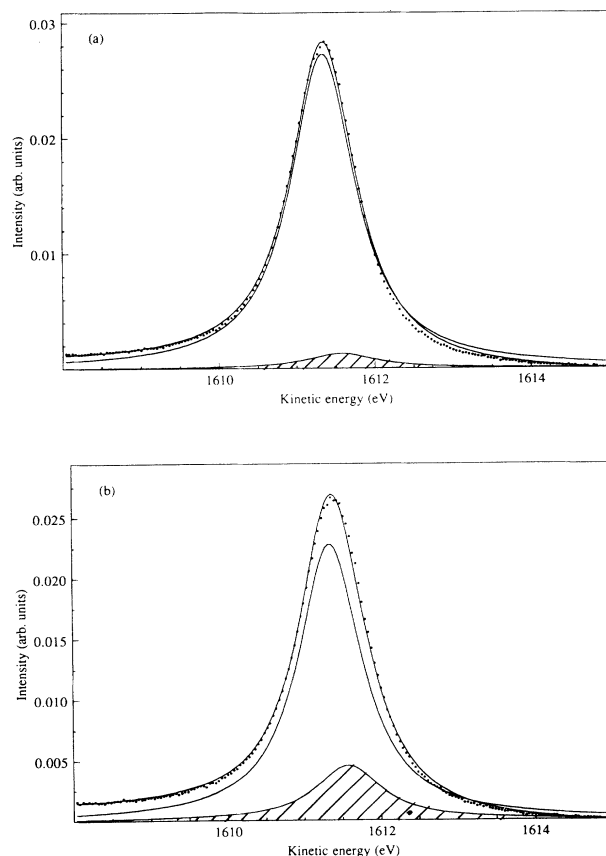


FIG. 5. Experimental spectra of the 1D component of the Si KLL Auger transition (dots) and the theoretical fit (line), for an angle between the surface and the direction of the electron lens of (a) 85° and (b) 15° . The positions and relative intensities of the components, without correction for the instrumental broadening, are shown with the component due to the interface shaded.

IV. DISCUSSION

As discussed in previous work,^{15–17,25} the change in the Auger parameter between two different environments $\Delta\alpha$ can be related to parameters linking the potential in the atomic core with changes in the valence charge and local environment according to

$$\Delta\alpha = \Delta \left[q \left(\frac{dk}{dN} \right) + \left[k - 2 \frac{dk}{dN} \right] \left(\frac{dq}{dN} \right) + \frac{dU}{dN} \right], \quad (3)$$

where q is the valence charge, k is the change in the core potential when a valence electron is removed, N is the occupation number of core orbitals, and U is the contribution to the core potential made by the atomic environment. In this expression the first term represents the relaxation contribution arising from shrinkage of the occupied valence orbitals when the atom is core-ionized; the second term represents the contribution from the transfer of screening charge from the environment to the valence orbitals of the core ionized atom; and the third term gives the effect of polarization of the surroundings by the core hole.

In the solid state, Si has incompletely filled 3s and 3p orbitals and any charge transfer occurring at the As/Si(100) interface might be expected to involve both valence orbitals. In consequence (3) is extended^{15,16} to a sum over unfilled orbitals i ,

$$\Delta\alpha = \Delta \sum_i \left[q_i \left(\frac{dk_i}{dN} \right) + \left[k_i - 2 \frac{dk_i}{dN} \right] \left(\frac{dq_i}{dN} \right) + \frac{dU}{dN} \right]. \quad (4)$$

For fully occupied valence orbitals such as the As 4s,²⁶ the initial-state charge transfer between two atomic envi-

ronments Δq_i will be zero, as will the valence charge attracted by core ionization dq_i/dN . There will thus be no change in this latter quantity between two environments and $\Delta(dq_i/dN)$ will also be zero.

In order to analyze the experimental results for the difference in Auger parameter $\Delta\alpha$ with a view to determining the charge transfer Δq between As/Si(100) and the pure elements, it is necessary to determine the values of the parameters k_i and their change with core occupancy dk_i/dN . The methods of determining these parameters from atomic structure calculations using the Dirac-Fock code of Desclaux²⁷ have been discussed in detail in earlier work^{15,16} and following the same procedures, which are outlined in the footnotes to Table II, we obtained the values for k_i and dk_i/dN for free As and Si atoms shown in Table II. The small errors quoted on the values of these parameters arise from different methods of calculating the parameters and from assuming different valence configurations for the free atoms.

Whereas the values of the potential parameters obtained from the free-atom calculations might be considered appropriate for the rather open structure at the As/Si(100) interface, we must consider the changes in the parameters brought about by compression of the valence wave functions in the elemental solids. Following previous work^{15,16} we allow for this compression by truncating the valence wave functions given by the Dirac-Fock calculations at a radius corresponding to the volume of the Wigner-Seitz cell and renormalizing the wave function within the cell. The values of the potential parameters corresponding to the renormalized or solid-state wave functions are also shown in Table II. Thomas and Weightman¹⁵ discuss the significance of this compression of the valence wave functions and conclude that the true potential parameters lie between the values found from

TABLE II. Theoretical estimates of potential parameters in eV.

	Free atom		Renormalized atom	
	a	b	c	d
	k_s	dk_s/dN	k'_s	dk'_s/dN
Si (2p;3s)	11.12±0.08	-2.64±0.05	11.79	-2.80
As (2p;4s)	11.62±0.02	-2.27±0.04	12.03	-2.35
	k_p	dk_p/dN	k'_p	dk'_p/dN
Si (2p;3p)	9.42±0.20	-3.17±0.03	11.21	-3.77
As (2p;4p)	9.80±0.03	-2.48±0.04	11.17	-2.83

^aFrom the difference in Koopmans's energy between a neutral and a valence-ionized atom. The uncertainties arise from slight differences in the results obtained for calculations of $[2p_{1/2}]$ and $[2p_{3/2}]$ hole states and for the assumption of different valence configurations: Si $3s^2 3p^2_{1/2}$, $3s^2 3p^2_{1/2}$; As $4s^2 4p^2_{1/2}$, $4p^2_{1/2}$, and $4s^2 3p^2_{3/2}$.

^bThe results quoted are the average of two different ways of calculating the parameters: $dk/dN = k_{\text{atom}} - k_{\text{core-ionized atom}}$ and $dk/dN = 2(k_{\text{atom}} - \Delta I)$, where $\Delta I = I_{\text{ion}} - I_{\text{atom}}$ and I_{atom} is the core-ionization energy determined from a difference in the total energy of the atom in its ground state and core-ionized state and I_{ion} is the corresponding quantity for an atom that has lost its outermost valence electron. The quoted uncertainties arise from the spread in the results obtained from these two different methods.

^c $k' = k(\langle 1/r \rangle_{rn} / \langle 1/r \rangle_{\text{atom}})$, where $\langle 1/r \rangle_{\text{atom}}$ and $\langle 1/r \rangle_{rn}$ are the expectation values for $1/r$ for atomic wave functions and wave functions that have been renormalized to the volume of the Wigner-Seitz cells, respectively.

^d $dk'/dN = (k'/k)(dk/dN)$.

free atom and renormalized calculations. Inspection of the values shown in Table II shows that the difference between the free atom and renormalized values of the parameters is far larger than the accuracy with which the free-atom parameters can be determined and we must consider this difference as an important limitation on the accuracy of this method of determining charge transfers. Qualitatively what we have to explain¹⁷ from the results in Table I is why core holes on Si atoms bonded to As atoms terminating a Si(100) surface are in a better screening environment than core holes in bulk Si ($\Delta\alpha = +0.68$ eV), while an As monolayer bonded to Si shows poorer core-hole screening than bulk As ($\Delta\alpha = -0.64$ eV). These observations may or may not reflect charge transfer at the interface. Let us consider some extreme views of what is going on.

A. The perfect local screening model

Equations (3) and (4) are greatly simplified for metallic environments¹⁵ since the screening of core-ionized sites is expected to be local. It is then reasonable to ignore the dU/dN term which represents the polarization of the environment accompanying core-hole formation and to assume that the screening of the core hole is complete and on site implying $dq/dN = 1$ in both environments so that $\Delta(dq/dN) = 0$. These assumptions make it possible to ignore the second and third terms in (3) and (4) and if we also ignore the difference in contributions arising from valence s and p electrons we are left with:

$$\Delta\alpha = \Delta q \left[\frac{dk}{dN} \right]. \quad (5)$$

It is instructive to apply this approximation, termed the "perfect local screening model" in an earlier¹⁶ application to PbTe, to the As/Si(100) system using values of dk/dN for each element averaged over the free atom and renormalized atom results for the s and p bonding orbitals (Table II). The data of Tables I and II yield charges on the interface atoms of $+0.26 \pm 0.05$ for As and -0.22 ± 0.05 for Si relative to the bulk elements. The experimental errors on these results are the sum of contributions of ~ 0.02 arising from the experimental error in determining $\Delta\alpha$ and ~ 0.03 due to the spread in values of the potential parameters. However, it must be emphasized that the main error in these estimates is likely to be associated with the inadequacies of the perfect local screening model in a semiconductor environment. Consequently, the prediction, to within the experimental accuracy, of equal and opposite charges on the As and Si atoms at the interface should be regarded as fortuitous.

We turn now to a more realistic treatment of the screening charge in the bulk elements and the interface which takes into account its more extended nature and the consequent contributions from the second and third terms in (3) and (4).

B. The imperfect screening model

Si is a semiconductor with a finite dielectric constant ($\epsilon = 12$), while As is a semimetal ($\epsilon \sim \infty$). The simple Jost

cavity model of Waddington *et al.*¹⁶ pictures the ionized atom in a spherical cavity of radius R in a medium of dielectric constant ϵ , and shows that the screening charge attracted to the cavity surface by a core hole at its center is $-(1-1/\epsilon)e$ rather than $-e$, as assumed above. This implies that the second and third terms of Eqs. (3) and (4) now assume importance. In the system discussed here the screening electrons are s - and p -like electrons. In the absence of d screening, which is important in transition metal compounds (see Veal and Paulikas²⁸ and Moretti and Porter²⁹), the Jost cavity screening will take approximate account of both additional terms. As has five valence electrons and, when bonded to Si, may significantly enhance the environmental screening at surface Si sites. Taking the extreme view that surface Si atoms are now perfectly screened, i.e., $^{Si}(1/\epsilon)_{Si(100)/As} \sim \infty$, so that $\Delta(dq/dN)$ is given by the screening of a Si site in bulk Si, $^{Si}(1/\epsilon)_{Si} \sim 0.08$. Then

$$\Delta\alpha \sim \Delta q \left[\frac{dk}{dN} \right] - ^{Si}(1/\epsilon)_{Si} \left[k - 2 \left[\frac{dk}{dN} \right] \right]. \quad (6)$$

Using average values of the k parameters (Table I) we now estimate $\Delta q = +0.23e$, i.e., the charge transfer is of opposite sign to that predicted in the perfect local screening model, but comparable in magnitude. Although we are here using a spherical cavity model for atoms only one layer below the surface, we can find some justification for this in Moretti's³⁰ emphasis on the importance of the nearest neighbors in the screening process.

Taking a similar extreme view of surface As screening we consider the consequences of surface As core holes being partly screened by Si electrons in an environment of reduced coordination. The combination of these two effects will reduce the effective surface dielectric constant. Ignoring the fact that the As environment is far from spherical, it is instructive to see the consequences of setting $^{As}(1/\epsilon)_{Si(100)/As} \sim 0.08$, i.e., comparable to bulk Si. Assuming screening by occupation of As $4p$ states leads to an estimate of $As^{-0.25}$, not inconsistent with the Si value above. Although the Jost cavity model is being applied beyond its immediate range of validity, we expect the consequences to be qualitatively right, i.e., tending towards $Si^{\delta+}As^{\delta-}$.

Given the disagreement in the sign of the initial-stage charge transfer between these two simple models, it is useful to develop an alternative estimate of charge transfer which is independent of screening assumptions. Measurements of the kind presented here make it possible to develop such an approach.

C. The initial-state viewpoint

The Auger parameter was created by Wagner³¹ to avoid energy referencing problems in electron spectroscopy. Following the notation of (1),

$$\Delta I \sim \Delta V + \Delta\phi - \Delta R, \quad (7)$$

$$\Delta K \sim -\Delta V - \Delta\phi + 3\Delta R, \quad (8)$$

where ΔV is the change in environmental potential at the emission site, $\Delta\phi$ the change in Fermi reference energy,

and ΔR the change in relaxation energy, all expressed relative to the elemental solid. It is customary to eliminate ΔV and $\Delta\varphi$ to give

$$\Delta\alpha = \Delta I + \Delta K = 2\Delta R; \quad (9)$$

however, we can equally well eliminate ΔR and define an initial-state parameter $\Delta\beta$

$$\Delta\beta = 3\Delta I + \Delta K = 2(\Delta V + \Delta\varphi). \quad (10)$$

Usually $\Delta\beta$ is a fairly useless parameter because the ΔV and $\Delta\varphi$ contributions cannot be separated, but in this work bulk Si and interface Si bonded to As were measured with the same energy reference so that for the Si results

$$\Delta\beta = 2\Delta V. \quad (11)$$

Such an inference is not possible for the As measurements since the reference levels of bulk As and As bonded to Si(100) will differ in a manner which is not readily determined. Isolation of ΔV in this way has previously been achieved for molecules,³² but here it is possible to apply the same separation of ΔV and ΔR at surfaces.

Following the ideas of Thomas and Weightman¹⁵ and others

$$\Delta\beta = 2\Delta q(k - M), \quad (12)$$

where Δq and k are as before and M represents a Madelung-style effect due to net charge on atoms in the surface layers. M is dependent on geometrical structure, but k and M will have the same sign so that ΔV will be much less than the bigger individual term. This implies that $\Delta\beta$ is similar to $\Delta\alpha$ in that it contains intra-atomic and extra-atomic contributions of opposite sign. Using optimized Si(100)/As structural parameters^{9,10,12} and assuming equal and opposite charges on the surface As layer and the top Si layer the Evjen method gives a Si Madelung potential per unit charge transfer $^{\text{Si}}M_{\text{Si}(100)/\text{As}} = 5.7$ eV/electron, a result which is relatively insensitive to local surface relaxation. Whatever k values are chosen from Table II ($k - M > 0$) so that the positive $\Delta\beta$ value obtained empirically (Table I) implies a positive Si initial-state charge. Using an averaged k value we estimate a Si surface charge $\Delta q_{\text{Si}} \sim +0.2e$, in accord with the imperfect screening model. It should be noted that the experimental $\Delta\beta$ values are much less accurate than the $\Delta\alpha$ because of the absence of the error compensation inherent in the determination of the Auger parameter shifts. The $\Delta\beta$ values for As yield no definitive information because of referencing problems, but if $\Delta\varphi$ is set to zero a negative charge of reasonable magnitude is predicted.

The models presented here do not provide unambiguous information about the charge transfer at interfaces, but they do highlight the main issues. The changes in $\Delta\alpha$ and $\Delta\beta$ both contain contributions from extra-atomic as well as intra-atomic effects and at complex interfaces quantitative estimates of interface screening are difficult to calculate. The present models are formulated in terms of charge transfer between atoms and it should be noted that in such covalently bonded systems it may be rehybridization rather than charge transfer that controls $\Delta\alpha$ and $\Delta\beta$. In this circumstance it may be necessary to develop some kind of bond charge model which takes account of the charge enhancement in chemical bonds. However, despite these reservations, the analysis of the photoelectron and Auger data obtained in this study does suggest a small positive charge transfer from As to Si ($\Delta q \sim 0.2e$). Our analysis indicates that this represents something close to the minimum charge that can be identified at semiconductor interfaces without much more sophisticated modeling. In metal alloys¹⁵ smaller charge transfers may be isolated because the systems conform more closely to the perfect screening viewpoint.

V. SUMMARY

The shift in photoelectron energy ΔI and Auger energy ΔK relative to the bulk elemental solid have been measured for both As and Si at the Si(100)/As interface. The respective changes in the Auger parameter are shown to be of opposite sign and indicate¹⁷ that core holes on Si atoms bonded to As at the interface are in a better screening environment than core holes in bulk Si, while an As monolayer bonded to Si shows poorer core-hole screening than bulk As. In addition for Si an initial state parameter $\Delta\beta = 3\Delta I + \Delta K$ is shown to be twice the change in local environment potential ΔV . Simple models for $\Delta\alpha$ and $\Delta\beta$ incorporating a balance of intra-atomic and extra-atomic contributions suggest a small positive charge transfer from As to Si, a result contrary to the simplistic perfect local screening viewpoint. Although it may be possible to recast some of the effect in terms of charge redistribution in dominantly covalent bonds, the present study shows how combining Auger and photoelectron data can separate initial- and final-state effects and so give more insight into electron redistribution at the surface than a photoemission study along.

ACKNOWLEDGMENTS

We wish to thank Catherine Baker for her help in evaluating Madelung potentials. This work was supported by the EC ESPRIT basic research action No. 3177, "EPIOPTIC."

¹J. R. Patel, P. E. Freeland, M. S. Hybertsen, and D. C. Jacobson, *Phys. Rev. Lett.* **59**, 2180 (1987).

²R. D. Brigans, M. A. Olmstead, R. I. G. Uhrberg, and R. Z. Bachrach, *Phys. Rev. B* **36**, 9569 (1987).

³H. Okumura, Y. Suzuki, K. Miki, K. Sakamoto, T. Sakamoto, S. Misawa, and S. Yoshida, *J. Vac. Sci. Technol. B* **7**, 481

(1989).

⁴Z. Sobiesierski, D. A. Woolf, D. I. Westwood, and R. H. Williams, *Mater. Sci. Eng. B* **5**, 275 (1990).

⁵J. Zegenhagen, J. R. Patel, B. M. Kincaid, J. A. Golovchenko, J. B. Mock, P. E. Freeland, R. J. Malik, and K.-G. Huang, *App. Phys. Lett.* **53**, 252 (1988).

- ⁶M. Copel and R. M. Tromp, *Phys. Rev. B* **37**, 2766 (1988).
- ⁷M. Copel, R. M. Tromp, and U. K. Köhler, *Phys. Rev. B* **37**, 10 756 (1988).
- ⁸J. R. Patel, J. Zegenhagen, P. E. Freeland, M. S. Hybertsen, J. A. Golovchenko, and D. M. Chen, *J. Vac. Sci. Technol. B* **7**, 894 (1989).
- ⁹R. I. G. Uhrberg, R. D. Brigans, R. Z. Bachrach, and J. E. Northrup, *Phys. Rev. Lett.* **56**, 520 (1986).
- ¹⁰R. I. G. Uhrberg, R. D. Brigans, R. Z. Bachrach, and J. E. Northrup, *J. Vac. Sci. Technol. A* **4**, 1259 (1986).
- ¹¹R. D. Brigans, R. I. G. Uhrberg, M. A. Olmstead, and R. Z. Bachrach, *Phys. Rev. B* **34**, 7447 (1986).
- ¹²R. D. Brigans, R. I. G. Uhrberg, M. A. Olmstead, R. Z. Bachrach, and J. E. Northrup, *Phys. Scr.* **T17**, 7 (1987).
- ¹³R. D. Brigans and M. A. Olmstead, *J. Vac. Sci. Technol. B* **7**, 1232 (1989).
- ¹⁴C. H. Patterson and R. P. Messmer, *Phys. Rev. B* **39**, 1372 (1989).
- ¹⁵T. D. Thomas and P. Weightman, *Phys. Rev. B* **33**, 5406 (1986).
- ¹⁶S. D. Waddington, P. Weightman, J. A. D. Matthew, and A. D. C. Grassie, *Phys. Rev. B* **39**, 10 239 (1989).
- ¹⁷J. A. D. Matthew, P. Weightman, and S. D. Waddington, *J. Phys. Condens. Matter* **1**, SB217 (1989).
- ¹⁸D. A. Woolf, D. I. Westwood, and R. H. Williams, *Semicond. Sci. Technol.* **4**, 1127 (1989).
- ¹⁹D. A. Woolf, D. I. Westwood, and R. H. Williams, *J. Cryst. Growth.* **108**, 25 (1991).
- ²⁰D. R. Penn, *J. Electron Spectrosc. Relat. Phenom.* **9**, 29 (1976).
- ²¹E. D. Roberts, P. Weightman, and C. E. Johnson, *J. Phys. C* **8**, 1301 (1975).
- ²²P. Weightman, E. D. Roberts, and C. E. Johnson, *J. Phys. C* **8**, 550 (1975).
- ²³E. J. McGuire, *Phys. Rev. A* **2**, 273 (1970).
- ²⁴E. J. McGuire, *Phys. Rev. A* **3**, 587 (1971).
- ²⁵T. D. Thomas, *J. Electron Spectrosc. Relat. Phenom.* **20**, 117 (1980).
- ²⁶X. Gonze, J.-P. Michenaud, and J.-P. Vigneron, *Phys. Rev. B* **41**, 11 827 (1990).
- ²⁷J. P. Desclaux, *Comput. Phys. Commun.* **9**, 31 (1975).
- ²⁸B. W. Veal and A. P. Paulikas, *Phys. Rev. B* **31**, 5399 (1985).
- ²⁹G. Moretti and P. Porta, *Surf. Interface Anal.* **15**, 47 (1990).
- ³⁰G. Moretti, *Surf. Interface Anal.* **16**, 159 (1990).
- ³¹C. D. Wagner, *Faraday Discuss. Chem. Soc.* **60**, 291 (1975).
- ³²E. J. Aitkin, M. K. Bahl, K. D. Bomben, J. K. Gimzewski, G. S. Nolan, and T. D. Thomas, *J. Am. Chem. Soc.* **102**, 4873 (1980).